AMERICAN ACADEMY OF OPHTHALMOLOGY®

Juvenile Batten Disease (*CLN3*): Detailed Ocular Phenotype, Novel Observations, Delayed Diagnosis, Masquerades, and Prospects for Therapy

Genevieve A. Wright, BSc,[1,2] Michalis Georgiou, MD,[1,2] Anthony G. Robson, PhD,[1,2] Naser Ali, FRCOphth,[1,2] Ambreen Kalhoro, FRCOphth,[2] SM Kleine Holthaus, PhD,[1] Nikolas Pontikos, PhD,[1,2] Ngozi Oluonye, MBBS,[2] Emanuel R. de Carvalho, PhD,[2] Magella M. Neveu, PhD,[1,2] Richard G. Weleber, MD,[3] Michel Michaelides, MD (Res), FRCOphth[1,2]

Purpose: To characterize the retinal phenotype of juvenile neuronal ceroid lipofuscinosis (JNCL), highlight delayed and mistaken diagnosis, and propose an algorithm for early identification.

Design: Retrospective case series.

Participants: Eight children (5 female) with JNCL.

Methods: Review of clinical notes, retinal imaging including fundus autofluorescence and OCT, electroretinography (ERG), and both microscopy and molecular genetic testing.

Main Outcome Measurements: Demographic data, signs and symptoms, visual acuity (VA), fundus autofluorescence and OCT findings, ERG phenotype, and microscopy/molecular genetics.

Results: Participants presented with rapid bilateral vision loss over 1 to 18 months, with mean VA deteriorating from 0.44 logarithm of the minimum angle of resolution (logMAR) (range, 0.20−1.78 logMAR) at baseline to 1.34 logMAR (0.30 logMAR - light perception) at last follow-up. Age of onset ranged from 3 to 7 years (mean, 5.3 years). The age at diagnosis of JNCL ranged from 7 to 10 years (mean, 8.3 years). Six children displayed eccentric fixation, and 6 children had cognitive or neurologic signs at the time of diagnosis (75%). Seven patients had bilateral bull's-eye maculopathy at presentation. Coats-like exudative vasculopathy, not previously reported in JNCL, was observed in 1 patient. OCT imaging revealed near complete loss of outer retinal layers and marked atrophy of the nerve fiber and ganglion cell layers at the central macula. An electronegative ERG was present in 4 patients (50%), but with additional a-wave reduction, there was an undetectable ERG in the remaining 4 patients. Blood film microscopy revealed vacuolated lymphocytes, and electron microscopy showed lysosomal (fingerprint) inclusions in all 8 patients.

Conclusions: In a young child with bilateral rapidly progressive vision loss and macular disturbance, blood film microscopy to detect vacuolated lymphocytes is a rapid, readily accessible, and sensitive screening test for JNCL. Early suspicion of JNCL can be aided by detailed directed history and high-resolution retinal imaging, with subsequent targeted microscopy/genetic testing. Early diagnosis is critical to ensure appropriate management, counseling, support, and social care for children and their families. Furthermore, although potential therapies for this group of disorders are in early-phase clinical trial, realistic expectations are that successful intervention will be most effective when initiated at the earliest stage of disease. *Ophthalmology Retina 2020;4:433-445 © 2019 by the American Academy of Ophthalmology. This is an open access article under the CC BY-NC-ND license (http://creativecommons.org/licenses/by-nc-nd/4.0/).*

Supplemental material available at www.ophthalmologyretina.org.

The neuronal ceroid lipofuscinoses (NCLs) are a group of inherited neurodegenerative lysosomal storage disorders that have been associated with 13 causative genes to date.[1] Prevalence is 1 in 100 000 live births.[2] Traditionally, the disease was divided into different forms dependent on the disease onset. Because disease onset and progression can vary substantially, genetic testing and confirmation of the underlying sequence variant are often required for a definite diagnosis. Consequently, a new gene-based nomenclature was introduced to facilitate disease classification.[3] Classic *CLN3* disease with juvenile disease onset, formerly known as "juvenile neuronal ceroid lipofuscinosis" (JNCL) and commonly referred to as "Batten disease," is a form of NCL caused by sequence

https://doi.org/10.1016/j.oret.2019.11.005
ISSN 2468-6530/19

variants in the gene *CLN3* (Ceroid Lipofuscinosis, Neuronal, 3; Online Mendelian Inheritance in Man: 204200). The gene codes for a transmembrane protein of unknown function.[4,5] Presentation is typically in early childhood with vision loss at 4 to 10 years of age, behavioral and cognitive dysfunction at 7 to 10 years of age, and progressive motor decline and seizures at 10 to 13 years of age, eventually leading to premature death in the second or third decade of life.[6,7] The most common sequence variant in *CLN3* is a homozygous 1 kb deletion, accounting for approximately 85% of cases of JNCL.[8,9] This deletion encompasses exons 7 to 8, resulting in a truncated, nonfunctional protein.[10] Other variants in *CLN3* can cause isolated adult-onset retinal degeneration.[11,12] Diagnosis of JNCL is confirmed by the presence of vacuolated lymphocytes and lysosomal (fingerprint) inclusions on blood film,[4,13–15] alongside molecular genetic testing.[3]

Visual impairment presents as the first symptom in more than 80% of cases of JNCL at a mean age of 5 years.[16,17] Retinal examination often shows a bull's-eye maculopathy, temporal optic disc pallor, peripheral retinal pigment epithelial disturbance (including bone spicule formation), and retinal vascular attenuation.[9,18–20] In one study, fundus imaging showed widespread atrophy of the retinal pigment epithelium (RPE) in 93% (n=24) of cases of confirmed *CLN3* disease.[21] However, because these retinal findings overlap with selected pathological hallmarks of more common disorders, including retinitis pigmentosa, Stargardt disease, and other inherited retinal diseases,[22–24] the early diagnosis of JNCL often results in significant diagnostic challenge. Furthermore, one clinical study reported only 2 of 9 patients with molecularly confirmed *CLN3*-JNCL as having bull's-eye maculopathy,[25] and another suggested that only 20% of cases present with a bull's-eye appearance, further highlighting the difficulties in early detection of JNCL.[21] Another less well-recognized clinical feature that can be seen in JNCL is "eccentric vision" or "overlooking," whereby the child will raise their eyes to overlook and fixate on a target object, and may be secondary to a relative degree of superior peripheral retinal sparing.[26]

The electroretinogram (ERG) is valuable in the diagnostic armamentarium for JNCL,[25] with marked ERG abnormalities invariably seen, including electronegative waveforms.[22,27,28] As the disease progresses to more advanced stages, the ERG shows significantly reduced cone responses and no recordable rod-specific responses.[18] Cognitive and behavioral impairment, in particular mood, memory, and attention (e.g., inability of the child to recall and accomplish 3-step commands), usually appears approximately 2 years after the onset of visual decline; however, these features may be present at first onset or occasionally in advance of visual symptoms, highlighting the importance of careful directed history in suspected cases.[16,17] Magnetic resonance imaging may show cerebral and cortical atrophy with demyelination.[29]

Timely diagnosis of JNCL is often challenging. Given the rapidly progressive and unfavorable prognosis of the disease, early diagnosis is important both to provide timely clinical management and support and to prepare for potential novel avenues of intervention. We describe 8 cases of JNCL presenting at a single tertiary referral center in detail, highlighting delayed/mistaken diagnosis and diagnostic challenges, providing diagnostic insights, novel observations, and recommendations. We discuss the latest research avenues being explored and ongoing or planned clinical trials.

Methods

Patient Identification

Patients with the diagnosis of JNCL and harboring likely disease-causing variants in *CLN3* were identified from the Moorfields Eye Hospital Inherited Eye Disease database. Patients were included in this database after obtaining informed consent. This retrospective study adhered to the tenets of the Declaration of Helsinki and was approved by the Moorfields Eye Hospital ethics committee.

Assessment

Medical notes and clinical images were reviewed, including dilated fundoscopy, visual acuity (VA), electrophysiologic testing (ERG), and retinal imaging, including OCT and fundus autofluorescence.

The age of disease onset was defined as the age at which the first disease-related symptom(s)/sign(s) were apparent. Screening for JNCL was done by microscopic evaluation of a peripheral blood film for the presence of vacuolated lymphocytes, followed by electron microscopy for storage (fingerprint) inclusions. Confirmation of the diagnosis was done by molecular genetic screening for *CLN3* variants.

Methods of electrophysiologic testing were adapted according to the age and ability of each individual to comply with testing. Full-field electroretinography (ERG) was performed to incorporate the International Society for Clinical Electrophysiology of Vision standards,[30] using a Ganzfeld bowl and gold foil corneal electrodes (case 7) or lower eyelid skin electrodes (case 6). The ERGs in the other children were performed with skin electrodes without mydriasis, using flashes delivered by a Ganzfeld bowl (cases 3, 5, and 8) or hand-held strobe (case 4), according to a modified protocol.[31] International Society for Clinical Electrophysiology of Vision standard pattern ERG[32] was performed using gold foil corneal (case 7) or skin electrodes.

The mean subfoveal choroidal thickness was measured by enhanced depth imaging horizontal OCT crosshair scans (Heidelberg Engineering Inc, Heidelberg, Germany). Segmentation of macular ganglion cell layer (mGCL) thickness was obtained using the automated segmentation software for the Spectralis OCT device (Heidelberg Engineering, software version 1.10.2.0). For retinal thickness maps, 3 circular lines representing 1, 3, and 6 mm scan diameters (Early Treatment Diabetic Retinopathy Study macula) were obtained. The macular scans were performed in the 30° perifoveal area using a 30°×25° OCT volume scan. The average of all points within the inner 1-mm diameter circle was defined as the central subfield thickness. The intermediate 3-mm ring was divided into the inner superior, inner nasal, inner inferior, and inner temporal subfields, and average values were calculated per sector in each eye.

Results

Clinical Findings

All 8 ascertained patients were first seen at Moorfields Eye hospital over a period of 8 years (2009–2017) and received the diagnosis of

Table 1. Clinical Features

	Case 1	Case 2	Case 3	Case 4	Case 5	Case 6	Case 7	Case 8
Sex	F	F	F	M	F	M	M	F
Age at onset (yrs)	5	5.5	3	7	4	6	6	6
Initial clinical findings at first evaluation	Macular atrophy, retinal degeneration on OCT	Nystagmus, reduced vision, poor night vision	Foveal thinning, optic disc pallor, bull's-eye maculopathy, poor color vision/night vision	Bilateral macular changes, optic disc pallor	Visual impairment	Noncorrectable vision, poor color vision	Unexplained poor vision	Esotropia, left amblyopia
VA; R, L (logMAR)	1.78, 1.78	0.60, 0.48	0.35, 0.80	0.60, 0.75	0.80, 0.80	0.70, 0.50	0.26, 0.20	0.18, 0.48
Neurologic/behavioral signs	Speech delay, clumsiness, seizures	None	Behavioral and cognitive decline (ASD?); clumsiness	Emotional difficulties, cognitive decline	None	None	Behavioral decline	Speech and language delay
Rapid visual decline within	6 mos	1 mo	12–18 mos	1 yr	12–18 mos	1 yr	1 yr	1 yr
Diagnosis on referral to Moorfields Eye Hospital	Severe retinal dystrophy	Severe retinal dystrophy	Molecularly confirmed Stargardt disease (*ABCA4*)	Severe retinal dystrophy	Unexplained vision loss	Unexplained vision loss	Unexplained vision loss	Unexplained vision loss
Age at diagnosis (yrs)	10	7	8	9	9	7	8	8
Clinical features at time of diagnosis	Profound macular atrophy, optic disc pallor, retinal vascular attenuation	Rotary nystagmus, pale optic discs, bull's-eye maculopathy, bilateral ERM, retinal vascular attenuation	Profound loss of inner and outer retina, bilateral ERM, bull's-eye maculopathy	Bilateral macular atrophy	Pale optic discs, attenuated vessels, bilateral macular atrophy	Loss of central retinal structure, bilateral ERM, poor color/night vision, pale optic discs	Bilateral ERM, outer retinal loss, pale optic discs	Bilateral macular atrophy, foveal sheen
VA; R, L (logMAR)	PL, PL	1.35, 1.60	1.20, 1.30	1.0, 1.10	1.30, 1.23	1.20, 1.20	0.50, 0.30	1.30, 1.30
Eccentric fixation/ overlooking	✓	✓	✓	NR	NR	✓	✓	✓
Neurologic/behavioral signs	Speech delay, clumsiness	None	Behavioral and cognitive decline, clumsiness	Cognitive decline	None	Clumsiness, memory loss, behavioral decline	Clumsiness, behavioral decline	Speech and language delay, poor concentration

ASD = autistic spectrum disorder; ERM = epiretinal membrane; L = left eye; logMAR = logarithm of the minimum angle of resolution; NR = not recorded; PL = perception of light; R = right eye.

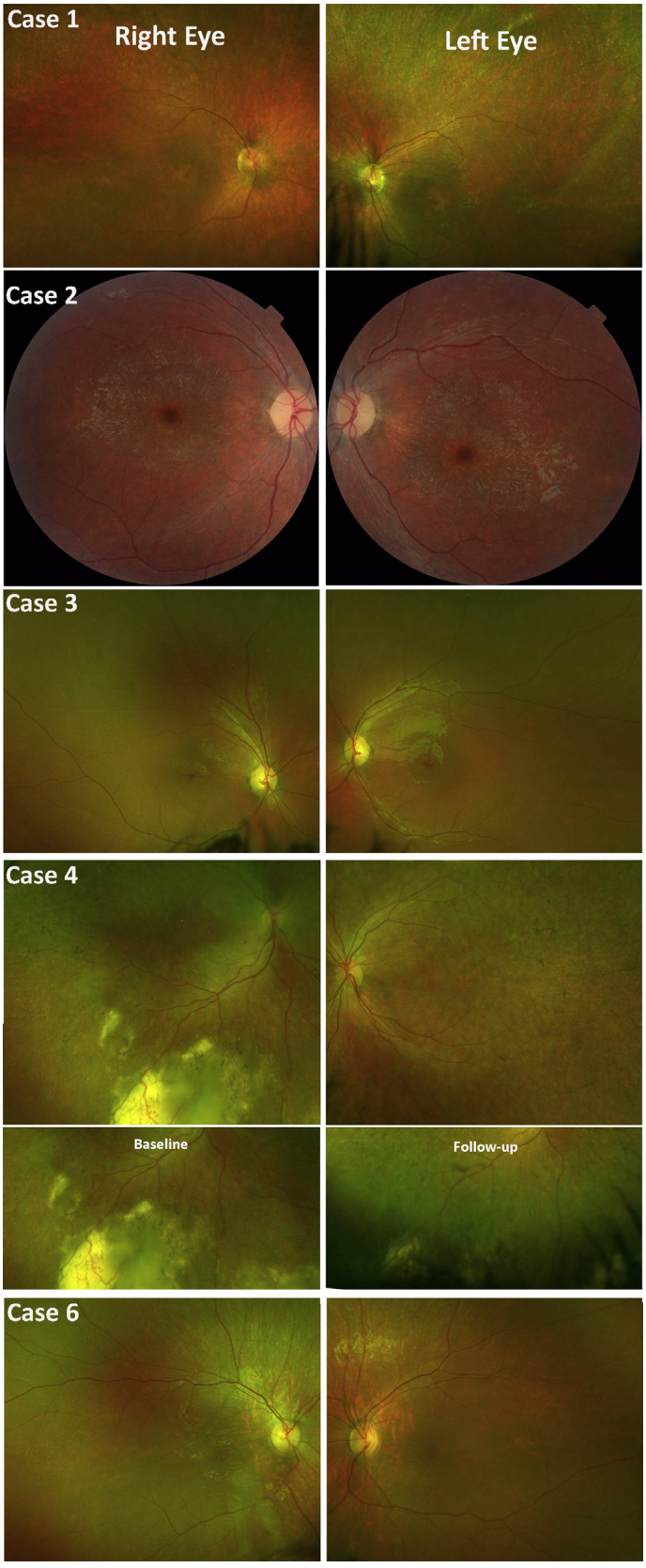

Figure 1. Clinical features on color fundus photography. Color fundus photographs of 5 cases with juvenile neuronal ceroid lipofuscinosis (JNCL) depicting optic disc pallor, macular atrophy with subtle granularity of the retinal pigment epithelium (RPE), and retinal arteriolar attenuation. Note the pigmentary changes reminiscent of bone spicules and unilateral Coats-like reaction in case 4. The second row for case 4 shows the exudation at baseline and its improvement over a follow-up period of 12 months.

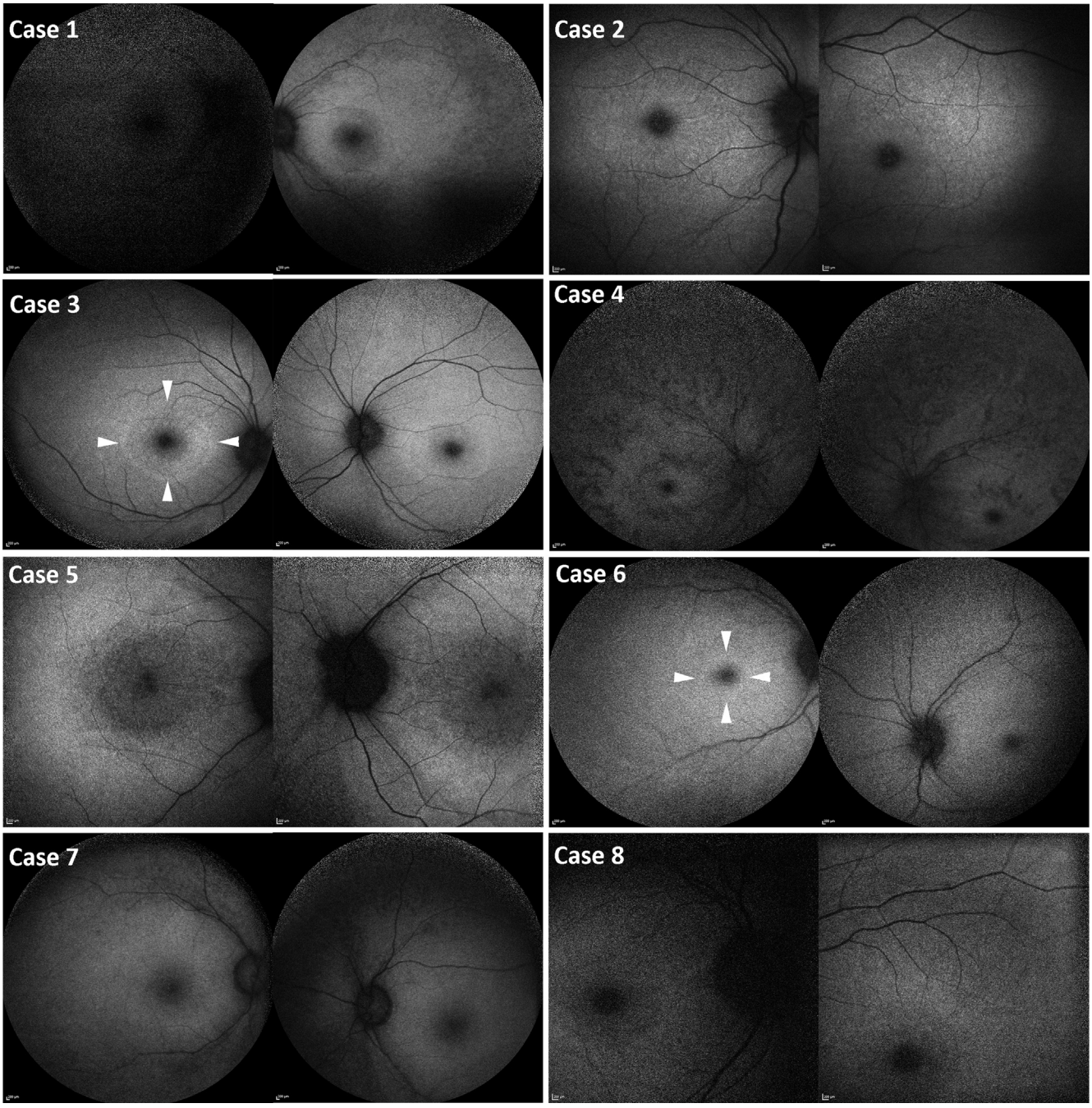

Figure 2. Fundus autofluorescence findings. Fundus autofluorescence images showing marked foveal hypoautofluorescence with varying degrees of surrounding diffuse reduction in macular autofluorescence. Cases 3 and 6: A ring of increased autofluorescence **(white arrowheads)**. Cases 3, 5, and 6 show mild diffuse peripheral hypoautofluorescence. Case 4 shows advanced diffuse hypoautofluorescence. Cases 1, 2, 7, and 8 show variable extent of decreased autofluorescence between the 2 groups.

CLN3 disease in 6 to 18 weeks after their first visit (mean, 10.7 weeks). They were referred with poor VA, with all having experienced a period of rapid visual decline before their referral to our tertiary center, ranging from 1 to 18 months in duration. Mean VA (±standard deviation [SD], range) at disease onset was 0.44 logarithm of the minimum angle of resolution (logMAR) (±0.44, 0.20−1.78 logMAR). Mean VA (±SD, range) by the time of diagnosis was 1.34 logMAR (±0.61, 0.30 logMAR - light perception). The age of disease onset ranged from 3 to 7 years (mean age, 5.3 years). The time from disease onset to diagnosis ranged from 1.5 to 5 years (mean time, 2.9 years). Age at diagnosis of JNCL ranged from 7 to 10 years (mean age, 8.3 years). The medical history before first presentation in 5 children was unremarkable (n=5, 62.5%), 1 patient had speech delay and learning

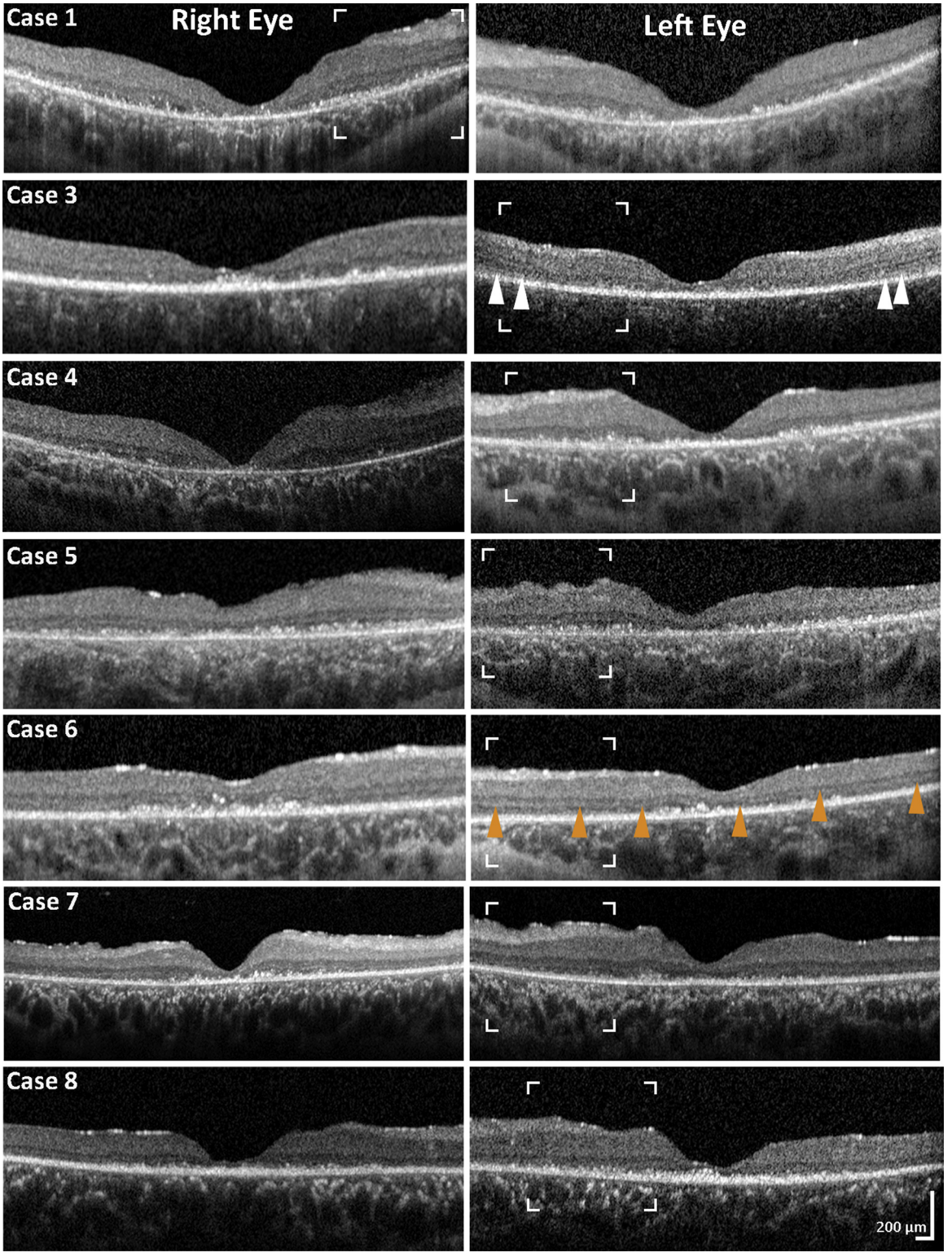

Figure 3. OCT findings. Spectral-domain OCT macular scans for all patients in the cohort, at the time of diagnosis, depicting significant macular atrophy with almost complete loss of the ellipsoid zone, hyper-reflective dots at the outer retinal level, and marked atrophy of the outer nuclear layer, outer plexiform layer, ganglion cell layer, and nerve fiber layer (NFL). Glial fibrosis is observed at the level of the inner retina. The **white arrowheads** mark possible areas of residual ellipsoid zone. The **orange arrowheads** mark an example of continuous, even though altered, external limiting membrane, despite the excessive loss of the photoreceptor layer. The white borders delineate regions of interest shown in greater magnification in Figure 4.

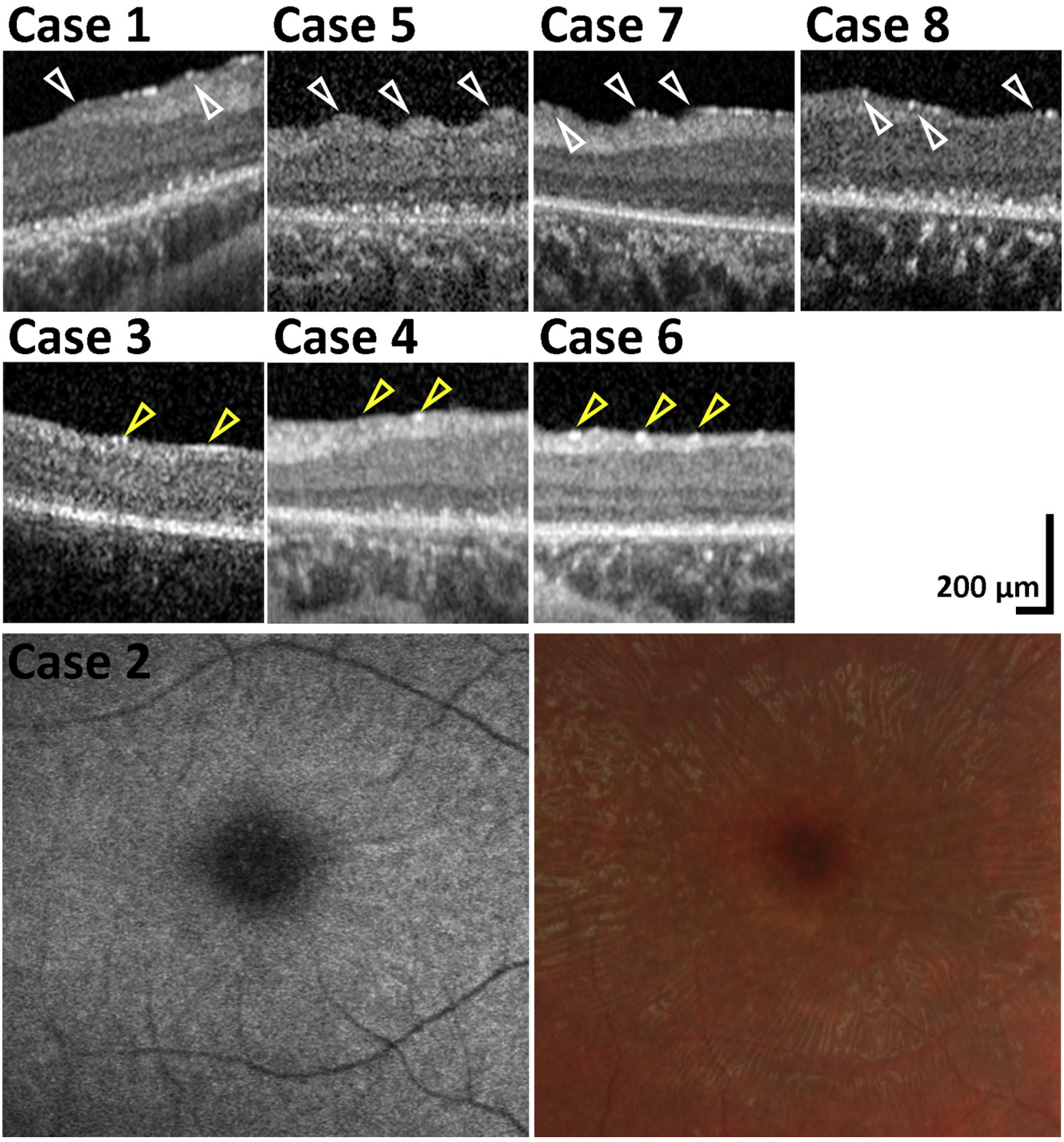

Figure 4. Macular striation and degenerative changes. Striation and degenerative changes were present in all patients. High magnification of the marked areas in Figure 3 is shown from horizontal OCT scans of the nasal fovea. Retinal radial striae within the vascular arcades were observed in cases 1, 5, 7, and 8. Striae resembled the appearance of epiretinal membranes (ERMs) on fundoscopy and color fundus photography, but no vessel alterations are seen and no definite membrane observed joining the tips, marked with **white arrowheads**, of the folds seen on OCT. Foci of increased signal, marked with **yellow arrowheads**, were observed in cases 3, 4, and 6 who did not have folds in contrast to a case with folds, where the areas of increased signal were greater in size and had a more linear distribution.

difficulties, and 1 patient had been hospitalized aged 8 weeks with hypoglycemia and low cortisol. Table 1 summarizes the clinical findings.

Six of 8 children were seen by an ophthalmologist at their local hospital before referral to our tertiary center (n=6, 75%). The other 2 cases (cases 6 and 7) were referrals from an orthoptist and

General Practitioner, respectively. In 3 cases (n=3, 37.5%, cases 2, 5, and 7), legal guardians had reported concerns about vision from as early as 3 years of age (range, 3−7). In 2 cases (cases 2 and 4), teachers had reported visual disturbance. At the time of referral, the presumed diagnoses in the 8 cases were Stargardt disease (n=1), severe retinal dystrophy (n=3), and unexplained visual loss (n=4) (Table 1).

Of note, 6 of 8 patients had eccentric fixation/"overlooking" (75%) either on observation or directed history. On directed detailed history, 6 of 8 patients had cognitive or neurologic signs (75%), including change in mood, behavior, balance, or memory. Magnetic resonance imaging was carried out in 3 children, and results were unremarkable.

Retinal Imaging

As shown in Figure 1, all but 1 patient (case 7) presented with a bull's-eye maculopathy. Optic disc pallor, arteriolar attenuation, and subtle granularity of the RPE were observed in all cases. Case 4 also developed inferior peripheral exudation, in keeping with a Coats-like vasculopathy (not previously reported in JNCL), which spontaneously improved over 12 months (Fig 1), and a mild mid-peripheral pigmentary retinopathy with bone spicule formation.

Macular fundus autofluorescence images (Fig 2) depict marked foveal hypoautofluorescence with varying degrees of surrounding diffuse reduction in macular autofluorescence in all patients (n=8, 100%). In addition, a perifoveal ring of increased autofluorescence was present in cases 3 and 6. Peripheral autofluorescence was variably decreased among the patients, ranging from mildly diffuse hypoautofluorescence (cases 3, 5, and 6) to markedly diffuse hypoautofluorescence (case 4). Cases 1, 2, 7, and 8 show variable extend of decrease autofluorescence between the 2 aforementioned groups. In cases 1 and 7, mild RPE mottling was seen in the periphery (Fig 2). In case 4, striae of decreased signal were observed in the periphery and perifoveal area (Fig 2).

OCT was available for analysis in 7 cases. In all cases, OCT imaging revealed near complete loss of photoreceptor cells, atrophy of the outer nuclear layer, outer plexiform layer, and marked atrophy of the nerve fiber and ganglion cell layers (Fig 3). The ellipsoid zone was markedly disrupted/absent, and it was difficult to identify remnants of the photoreceptor layer because of debris. Hyper-reflective dots were visible at the level of the expected photoreceptor layer (Fig 3).

Mean subfoveal choroidal thickness was within age-adjusted normal limits (mean, 336 μm right eye and 330 μm left eye). Automated segmentation of the mGCL was performed in 4 patients (cases 1, 3, 4, and 6). The values obtained from the 1-mm diameter central subfield area were excluded from analysis because the mGCL in the central subfield was very thin, precluding adequate segmentation. The values corresponding to the 6-mm outer ring were excluded because they fell outside the scanning area as the result of eccentric fixation. The average mGCL of the intermediate 3-mm ring was 10.84 μm (SD±2.87 μm) (Supplementary Fig 1, available at www.ophthalmologyretina.org). The average mGCL thickness was 44.1±9.22 μm, with a mean (5th−95th percentile) normative value for children aged 5 to 17 years (n=276) of 51.6 μm (44.43−58.25 μm).[33]

In addition to mGCL thinning, changes at the level of nerve fiber layer (NFL) and internal limiting membrane (ILM) were observed in all patients. Radial retinal striae were observed within the vascular arcades in 5 cases (n=5, 62.5%, Figs 3 and 4). Striae (folds) resembling epiretinal membranes (ERMs), but without vessel alterations, were seen on fundoscopy and color fundus photography (Fig 4, case 2). No definite membrane was seen joining the tips of the folds on OCT (Fig 4, cases 1, 5, 7, and 8). In contrast, gliosis of the inner retina, presented as increased reflectivity at the ILM,[34] was evident in all but 1 patient (case 3). An increased, patchy (linear) signal observed at the level of the ILM with severe disruption of the NFL appears to have led to more prominent "folding" nasally, possibly related to greater NFL thickness (Fig 3). Foci of increased signal, instead of patchy linear areas, were observed in the 3 cases without folds (Fig 4, cases 3, 4, and 6). The external limiting membrane was present but disrupted (Fig 3), and no folds were present in these patients, perhaps representing an earlier stage of the disease. The mean age at the time of OCT imaging was 8.9 years for patients with striae and 8.0 years for patients without striae.

Electrophysiologic Assessment

Full-field and flash ERGs were recorded in all patients under photopic and scotopic conditions. Cases 1, 2, 4, and 5 had undetectable ERGs, in keeping with severe rod and cone photoreceptor dysfunction (Fig 5A). Cases 3, 6, 7, and 8 had undetectable scotopic dim flash ERGs; strong flash ERGs were electronegative but with additional a-wave reduction. The photopic single flash ERGs had a low b:a ratio but with additional a-wave reduction in cases 7 and 8. The light-adapted 30 Hz flicker ERGs were mildly delayed in all cases with a detectable response (cases 3, 6, 7, and 8) (Fig 5A and B). The findings were consistent with marked generalized inner retinal dysfunction of rod (cases 3, 6, 7, and 8) and cone (cases 7 and 8) systems, with additional rod and cone photoreceptor involvement in all cases. Pattern ERGs were undetectable in the 6 cases tested in keeping with severe macular dysfunction.

Blood Film Microscopy/Electron Microscopy

Blood film microscopy performed for all 8 patients demonstrated vacuolated lymphocytes. Electron microscopy was done sequentially in 7 patients, and all showed lysosomal (fingerprint) inclusions.

Molecular Genetics

All patients were molecularly confirmed as harboring likely disease-causing variants in *CLN3*. Six of 8 patients were homozygous for the common 1.02 kb deletion. Case 8 was homozygous for c.(962+dup). Case 7 was compound heterozygotes for c.(1056+3A>C) and deletion of exons 2−5. One patient (case 3) was initially referred with molecularly confirmed Stargardt disease for consideration of clinical trials/studies. The clinical presentation/detailed history/imaging was not in keeping with Stargardt disease, and so investigation was initiated for JNCL. The previously identified compound heterozygous *ABCA4* variants were further assessed in silico, with one of the variants determined to be unlikely to be pathogenic. Determination of disease causation of

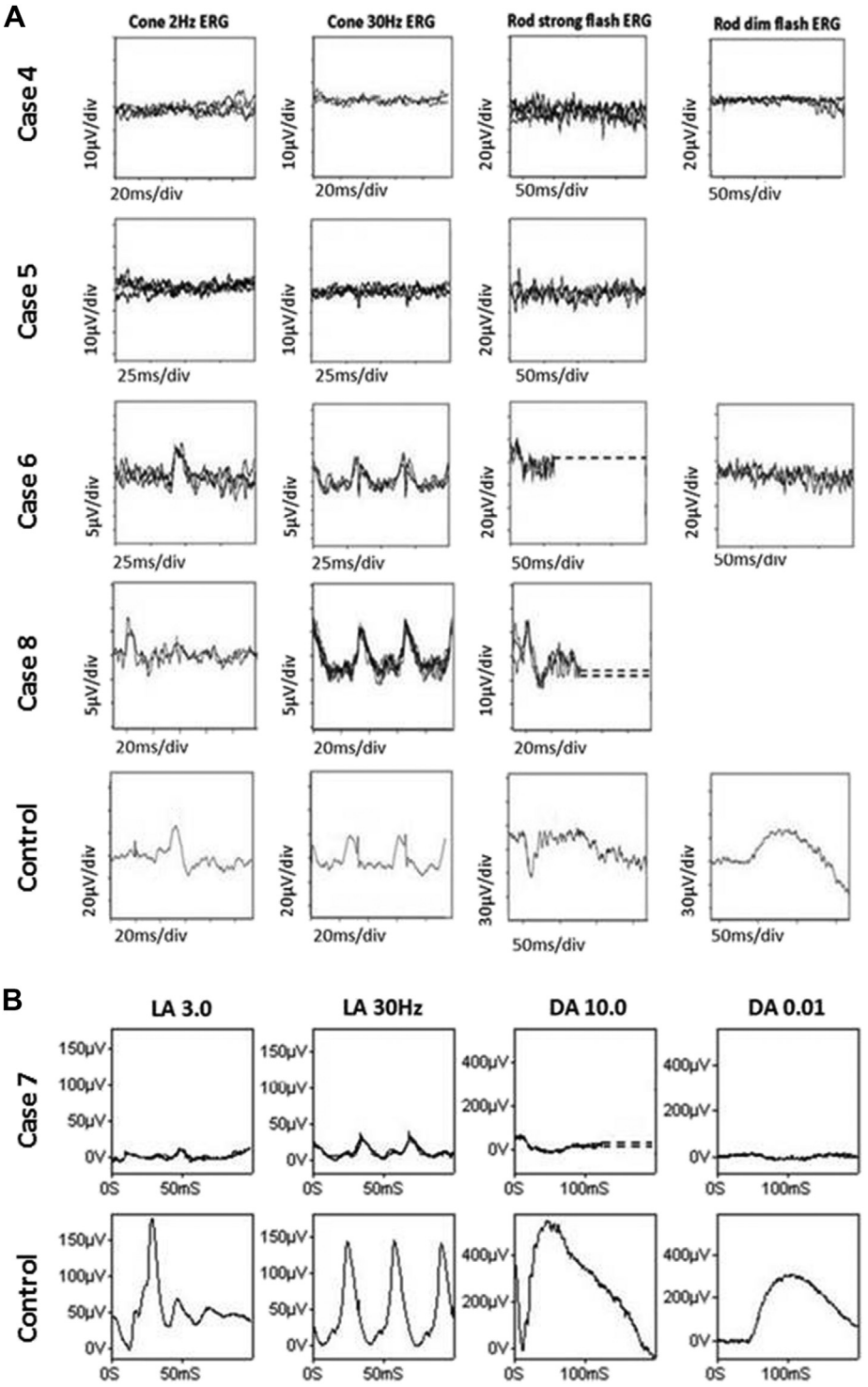

Figure 5. Electroretinography (ERG) recorded with lower eyelid skin electrodes in cases 4, 5, 6, and 8 (**A**) and with corneal electrodes in case 7 (**B**). Note 20 ms prestimulus delay in single flash ERGs. Electrode-specific control recordings are shown for comparison but without a 20 ms prestimulus delay in **B**. International Society for Clinical Electrophysiology of Vision standard stimuli were used in case 4 (without mydriasis), and in cases 6 and 7 a strobe was used to deliver flashes in subjects unable to comply with Ganzfeld testing (dim flash rod ERG/DA0.01 ERG excluded from the protocol). International Society for Clinical Electrophysiology of Vision standard testing (cases 6 and 7) included the dark-adapted (DA) ERGs (flash strengths 0.01 and 10.0 cd.s/m2; DA 0.01 and DA 10.0) and light-adapted (LA) ERGs for a flash strength of 3.0 cd.s/m2 (LA 3.0; 30 Hz and 2 Hz). Data are shown for 1 eye, but all had symmetrical responses. Broken lines replace blink/eye movement artefacts occurring after ERG b-waves for clarity. Recordings from patients are superimposed to demonstrate reproducibility. Note the small differences in scaling and format of skin ERGs **(A)** related to use of different recording equipment. See text for ERG analysis.

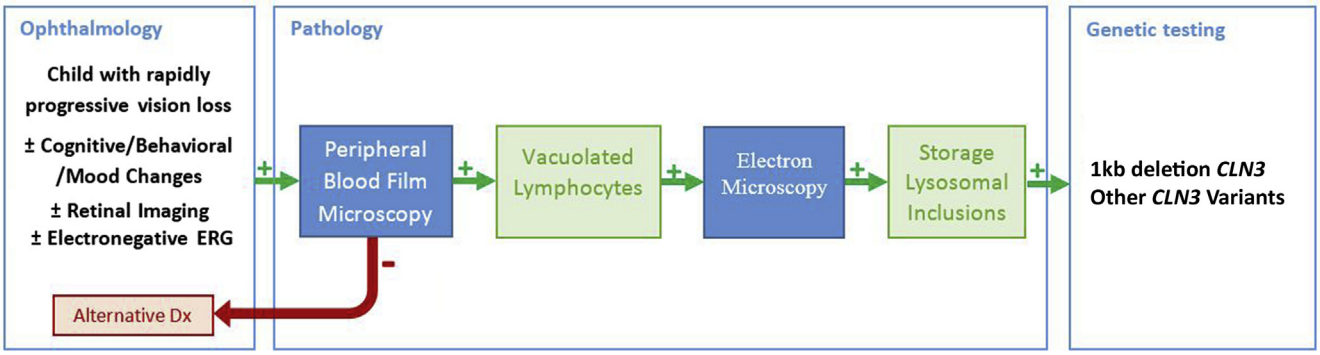

Figure 6. Diagnostic algorithm for JNCL, *CLN3*-associated disease. In a child with bilateral rapidly progressive vision loss, microscopy of peripheral blood film can detect the presence of vacuolated lymphocytes, a sensitive screening test for JNCL, followed by electron microscopy for lysosomal storage inclusions. Confirmation of the diagnosis should follow with molecular genetic testing for *CLN3* variants. ERG = electroretinography.

ABCA4 variants is highly challenging given the vast allelic heterogeneity and highly polymorphic nature of this large gene.

Discussion

This report characterizes the early retinal phenotype of juvenile Batten disease, highlights the importance of early diagnosis of *CLN3* disease in young children who present with rapid visual loss, with or without the presence of neurologic or cognitive symptoms, and describes conditions that can masquerade as *CLN3* disease.

Our case series identified a significant delay in diagnosis in all 8 children, with an average delay of 2.9 years from first presentation to diagnosis, in line with previous studies reporting a delay of 1.3 to 4 years.[9,25] It is of note that in the past, the diagnosis was often only made after the onset of seizures despite prior visual failure,[26] whereas early diagnosis should now be possible after the advancements in retinal imaging and molecular testing that are now readily available.

There are several clinical symptoms (likely to require a directed careful history, including eccentric viewing and changes in mood/behavior/cognition/memory) and signs on examination/detailed imaging that should warrant directed investigations to promptly diagnose *CLN3*-JNCL. These include visual loss, which is characteristically rapid, and was present in all of our cases, most commonly reported in the literature in those aged 6 to 8 years.[9,11,25,28] Other associated behavioral and cognitive impairments were also present in 6 of 8 cases; however, these were often not identified at the time of visual symptoms or not investigated or considered pertinent to the unexplained/otherwise explained visual loss, thereby further contributing to delayed diagnosis.

Fundus abnormalities seen in *CLN3* disease such as "bull's-eye" maculopathy, retinal vascular attenuation, and optic disc pallor were present in our series, but these are also features of other severe retinopathies.[23,24] Previously, eccentric fixation or "overlooking" has been attributed to a degree of superior peripheral retinal sparing.[26] Despite the majority of the patients in our study having eccentric fixation/overlooking (Table 1), the disease appeared relatively symmetrical between the superior and inferior retina on fundus autofluorescence imaging (Fig 3), suggesting no obvious anatomic difference and no functional difference (indirectly), although we cannot exclude that *direct* functional testing may identify a difference between superior and inferior retinal sensitivity.

Abnormalities in OCT features can be helpful in guiding the clinician to directly investigate *CLN3*-disease, including the profound degree and extent of outer retinal loss of lamination at a relatively young age, significant inner retinal thinning, and the presence of increased inner retinal reflectivity. The increased reflectivity has been described as being secondary to ERM formation in several reports. Hainsworth et al[21] identified ERM in 33% of their cohort (n=24) on the basis of fundus appearance alone. More recently, Dulz et al[9] described a striation pattern without ERM in all their patients (n=11, mean age 14.4 years) using OCT. In our cohort, all patients had reflectivity changes in the NFL and ILM. Although the mean age of our cohort was lower (average age 8.9 years), retinal striation was observed in 62.5% of the patients, distinct from typical ERM, with the 3 patients without striae being on average 1 year younger (8 years) (Fig 4). Our findings of profound diffuse macular ganglion cell thinning are in keeping with the degenerative NFL and mGCL loss reported in histologic studies.[35,36]

The scotopic ERGs in 4 of 4 cases with a detectable response had electronegative waveforms, consistent with dysfunction that is postphototransduction or inner retinal, but with a-wave reduction indicating significant additional loss of photoreceptor function. An electronegative ERG has often been associated with juvenile *CLN3* disease and may prompt screening in some cases, particularly if the photopic ERG shows a reduced b:a ratio.[25] However, it is noted that an electronegative ERG is not diagnostic and is a feature of congenital stationary night blindness, X-linked retinoschisis, and many other disorders.[22,37–39]

One patient was initially referred with molecularly confirmed Stargardt disease for consideration of clinical trials/studies. The clinical presentation/detailed history/imaging was not entirely typical of Stargardt disease, and

investigation was initiated for JNCL. The previously identified compound heterozygous *ABCA4* variants were further assessed in silico, with one of the variants determined unlikely to be pathogenic. Determination of disease-causation of *ABCA4* variants is highly challenging given the vast allelic heterogeneity and highly polymorphic nature of this large gene. This case highlights (1) that the clinician needs to be mindful that severe *ABCA4*-retinopathy associated with generalized cone-rod dystrophy at an early age can masquerade as *CLN3*-JNCL; (2) the difficulties in definitively ascribing disease causation to identified sequence variants in this era of genomic ophthalmology and more readily accessible genetic testing; and (3) further illustrates the challenges in diagnosing *CLN3* disease in a timely fashion and the potential consequences of mistaken diagnosis.

Early diagnosis of JNCL remains a diagnostic challenge, particularly because other severe retinal dystrophies can present with early-onset visual loss. Moreover, associated nonocular symptoms/signs are often compartmentalized and investigated separately, which can lead to further delay. We suggest that a child with bilateral rapidly progressive vision loss, with or without cognitive/behavioral problems at presentation, should have microscopy of a peripheral blood film to detect the presence of vacuolated lymphocytes, which can act as a sensitive screening test (all patients with *CLN3* disease will test positive), followed by electron microscopy for storage (fingerprint) inclusions.[15] Diagnostic confirmation should be done with molecular genetic screening of *CLN3* (Fig 6).

The most common variant in *CLN3*-JNCL is a 1 kb deletion resulting in a frameshift and truncated protein product.[10] In our cohort, 75% of cases were homozygous for this deletion and had similar clinical presentations. Case 8, who harbored the c.(962+dup) variant homozygously, was reported to have better VA at presentation, but by the time of diagnosis had similar VA to the other patients. Case 7, the only compound heterozygote in our cohort (c.(1056+3A>C) and deletion of exon 2−5), had a milder ocular phenotype, with the most preserved VA in the cohort and a degree of residual ellipsoid zone on OCT (Fig 3). Because this patient presented with early cognitive and behavioral abnormalities, it could be speculated that this genetic variant may have less deleterious effects on vision. Case 7 also had electronegative ERGs but with an altered waveform morphology of the rod ERG, which was not observed in any of the other subjects. The significance of this ERG finding is uncertain. Although there is no treatment that has been shown in a clinical trial to benefit patients with JNCL, it is important to explain the genetics of the disease to the parents, provide genetic counseling, offer to follow the child yearly for routine eye care, and offer to refer them to a pediatric neurologist, knowledgeable pediatrician, or family practitioner who is willing and able to help follow and care for the child. This includes specialist knowledge of certain medications that are more likely to induce adverse side effects when given to a child with JNCL. Referral to international foundations that support research on the NCL disorders, social workers, or local or national support groups of parents who have children with JNCL may help parents and families cope with issues commonly seen as the disease progresses.

To date, there are no treatments available for juvenile *CLN3* Batten disease or other forms of NCL. The majority of studies has focused on developing therapeutic interventions to combat the neurodegeneration in NCL, including enzyme replacement therapy, gene therapy, stem cell transplantation, and pharmacologic approaches.[40,41] Most notably, patients with *CLN2* disease who received biweekly intraventricular infusion of soluble CLN2 enzyme (NCT01907087, NCT02485899) showed no significant decline in motor or language skills, and overall disease progression was considerably slowed during the reporting period.[41] The treatment has now received Food and Drug Administration and European Medicines Agency approval. A phase I/II trial has also started for *CLN6* disease using gene therapy administered by a single intrathecal injection of adeno-associated virus 2/9 carrying *CLN6* (NCT02725580). This study is ongoing, but data from 8 of 12 patients 2 years after vector injection are available and show promising preliminary results. On the basis of these data, a phase I/II clinical trial has started recruiting for *CLN3* disease to investigate intrathecally administered AAV2/9-*CLN3* (NCT037770572). Although these studies will primarily assess treatment safety and effects on neurologic features, they may also help to determine whether brain-directed gene therapy has any impact on vision in *CLN6* and *CLN3* cases. Because *CLN6* and *CLN3* encode membrane-bound proteins that are not passed on to neighboring cells, it is more likely that gene therapy directly targeting the eye will be more effective to prevent retinal degeneration in both diseases. A proof-of-concept study demonstrated that ocular gene therapy is therapeutic in *Cln6*^{nclf} mice, a mouse model for *CLN6* disease, when the inner retina was treated.[41] Preclinical ocular gene therapy for *CLN3* disease has not been described yet. However, a similar gene therapy approach targeting the cells of the inner retina as used in *Cln6*^{nclf} mice could be effective in *Cln3*-deficient mice[25] and may be relevant to human *CLN3* disease (both syndromic and nonsyndromic).

Conclusions

We have described cases of juvenile *CLN3* disease in detail, highlighting delayed or mistaken diagnosis and diagnostic challenges; providing diagnostic insights, novel observations, and recommendations; and highlighting the latest clinical research and ongoing/planned clinical trials. We have also emphasized the role of the ophthalmologist and pediatrician or primary care provider and the need for additional continued support for the family. Although timely diagnosis of JNCL is often challenging, given the rapidly progressive and unfavorable prognosis of the disease, early diagnosis is important both to provide timely clinical management and support and to facilitate access to novel therapeutic interventions at the early disease stages.

Acknowledgment. The authors thank Drs. Glen Anderson and Clare Beesley, at the Camelia Botnar Laboratory/Molecular Genetics Laboratory, Great Ormond Street Hospital, for their efficient and timely diagnostic screening service for JNCL-*CLN3*.

References

1. Johnson TB, Cain JT, White KA, et al. Therapeutic landscape for Batten disease: current treatments and future prospects. *Nat Rev Neurol*. 2019;15:161−178.
2. Isolation of a novel gene underlying Batten disease, CLN3. The International Batten Disease Consortium. *Cell*. 1995;82:949−957.
3. Williams RE, Mole SE. New nomenclature and classification scheme for the neuronal ceroid lipofuscinoses. *Neurology*. 2012;79:183−191.
4. Licchetta L, Bisulli F, Fietz M, et al. A novel mutation af Cln3 associated with delayed-classic juvenile ceroid lipofuscinois and autophagic vacuolar myopathy. *Eur J Med Genet*. 2015;58:540−544.
5. Mole SE, Williams RE. Neuronal ceroid-lipofuscinoses. In: Adam MP, Ardinger HH, Pagon RA, et al., eds. GeneReviews((R)). Seattle, WA: University of Washington, Seattle.
6. Schultz ML, Tecedor L, Chang M, Davidson BL. Clarifying lysosomal storage diseases. *Trends Neurosci*. 2011;34:401−410.
7. Mink JW, Augustine EF, Adams HR, et al. Classification and natural history of the neuronal ceroid lipofuscinoses. *J Child Neurol*. 2013;28:1101−1105.
8. Mole SE. The genetic spectrum of human neuronal ceroid-lipofuscinoses. *Brain Pathol*. 2004;14:70−76.
9. Dulz S, Wagenfeld L, Nickel M, et al. Novel morphological macular findings in juvenile CLN3 disease. *Br J Ophthalmol*. 2016;100:824−828.
10. Jarvela I, Autti T, Lamminranta S, et al. Clinical and magnetic resonance imaging findings in Batten disease: analysis of the major mutation (1.02-kb deletion). *Ann Neurol*. 1997;42:799−802.
11. Mole SE, Williams RE, Goebel HH. Correlations between genotype, ultrastructural morphology and clinical phenotype in the neuronal ceroid lipofuscinoses. *Neurogenetics*. 2005;6:107−126.
12. Ku CA, Hull S, Arno G, et al. Detailed clinical phenotype and molecular genetic findings in CLN3-associated isolated retinal degeneration. *JAMA Ophthalmol*. 2017;135:749−760.
13. Santavuori P. Neuronal ceroid-lipofuscinoses in childhood. *Brain Dev*. 1988;10:80−83.
14. Kousi M, Lehesjoki AE, Mole SE. Update of the mutation spectrum and clinical correlations of over 360 mutations in eight genes that underlie the neuronal ceroid lipofuscinoses. *Hum Mutat*. 2012;33:42−63.
15. Anderson G, Smith VV, Malone M, Sebire NJ. Blood film examination for vacuolated lymphocytes in the diagnosis of metabolic disorders; retrospective experience of more than 2,500 cases from a single centre. *J Clin Pathol*. 2005;58:1305−1310.
16. Cialone J, Adams H, Augustine EF, et al. Females experience a more severe disease course in Batten disease. *J Inherit Metab Dis*. 2012;35:549−555.
17. Marshall FJ, de Blieck EA, Mink JW, et al. A clinical rating scale for Batten disease: reliable and relevant for clinical trials. *Neurology*. 2005;65:275−279.
18. Ostergaard JR. Juvenile neuronal ceroid lipofuscinosis (Batten disease): current insights. *Degener Neurol Neuromuscul Dis*. 2016;6:73−83.
19. Eksandh LC, Ponjavic V, Ayyagari R, et al. Phenotypic expression of juvenile X-linked retinoschisis in Swedish families with different mutations in the XLRS1 gene. *Arch Ophthalmol*. 2000;118:1098−1104.
20. Bensaoula T, Shibuya H, Katz ML, et al. Histopathologic and immunocytochemical analysis of the retina and ocular tissues in Batten disease. *Ophthalmology*. 2000;107:1746−1753.
21. Hainsworth DP, Liu GT, Hamm CW, Katz ML. Funduscopic and angiographic appearance in the neuronal ceroid lipofuscinoses. *Retina*. 2009;29:657−668.
22. Horiguchi M, Miyake Y. Batten disease–deteriorating course of ocular findings. *Jpn J Ophthalmol*. 1992;36:91−96.
23. Krohne TU, Herrmann P, Kopitz J, et al, [Juvenile neuronal ceroid lipofuscinosis. Ophthalmologic findings and differential diagnosis]. *Ophthalmologe*. 2010;107:606−611.
24. Bozorg S, Ramirez-Montealegre D, Chung M, Pearce DA. Juvenile neuronal ceroid lipofuscinosis (JNCL) and the eye. *Surv Ophthalmol*. 2009;54:463−471.
25. Collins J, Holder GE, Herbert H, Adams GG. Batten disease: features to facilitate early diagnosis. *Br J Ophthalmol*. 2006;90:1119−1124.
26. Spalton DJ, Taylor DS, Sanders MD. Juvenile Batten's disease: an ophthalmological assessment of 26 patients. *Br J Ophthalmol*. 1980;64:726−732.
27. Weleber RG. The dystrophic retina in multisystem disorders: the electroretinogram in neuronal ceroid lipofuscinoses. *Eye (Lond)*. 1998;12(Pt 3b):580−590.
28. Mantel I, Brantley Jr MA, Bellmann C, et al. Juvenile neuronal ceroid lipofuscinosis (Batten disease) CLN3 mutation (Chrom 16p11.2) with different phenotypes in a sibling pair and low intensity in vivo autofluorescence. *Klin Monbl Augenheilkd*. 2004;221:427−430.
29. Autti TH, Hamalainen J, Mannerkoski M, et al. JNCL patients show marked brain volume alterations on longitudinal MRI in adolescence. *J Neurol*. 2008;255:1226−1230.
30. McCulloch DL, Marmor MF, Brigell MG, et al. ISCEV Standard for full-field clinical electroretinography (2015 update). *Doc Ophthalmol*. 2015;130:1−12.
31. Holder G, Robson A. In: Lorenz B, ed. *Paediatric Electrophysiology: A Practical Approach. Essentials in Ophthalmology*. Berlin: Springer-Verlag; 2006:133−155.
32. Bach M, Brigell MG, Hawlina M, et al. ISCEV standard for clinical pattern electroretinography (PERG): 2012 update. *Doc Ophthalmol*. 2013;126:1−7.
33. Yoo YJ, Hwang JM, Yang HK. Inner macular layer thickness by spectral domain optical coherence tomography in children and adults: a hospital-based study. *Br J Ophthalmol*. 2019;103:1576−1583.
34. Preising MN, Abura M, Jager M, et al. Ocular morphology and function in juvenile neuronal ceroid lipofuscinosis (CLN3) in the first decade of life. *Ophthalmic Genet*. 2017;38:252−259.
35. Traboulsi EI, Green WR, Luckenbach MW, de la Cruz ZC. Neuronal ceroid lipofuscinosis. Ocular histopathologic and electron microscopic studies in the late infantile, juvenile, and adult forms. *Graefes Arch Clin Exp Ophthalmol*. 1987;225:391−402.
36. Goebel HH, Fix JD, Zeman W. The fine structure of the retina in neuronal ceroid-lipofuscinosis. *Am J Ophthalmol*. 1974;77:25−39.
37. Weleber RG, Gupta N, Trzupek KM, et al. Electroretinographic and clinicopathologic correlations of retinal dysfunction in infantile neuronal ceroid lipofuscinosis (infantile Batten disease). *Mol Genet Metab*. 2004;83:128−137.

38. Audo I, Robson AG, Holder GE, Moore AT. The negative ERG: clinical phenotypes and disease mechanisms of inner retinal dysfunction. *Surv Ophthalmol*. 2008;53:16–40.
39. Robson AG, Nilsson J, Li S, et al. ISCEV guide to visual electrodiagnostic procedures. *Doc Ophthalmol*. 2018;136:1–26.
40. Mole SE, Anderson G, Band HA, et al. Clinical challenges and future therapeutic approaches for neuronal ceroid lipofuscinosis. *Lancet Neurol*. 2019;18:107–116.
41. Schulz A, Ajayi T, Specchio N, et al. Study of intraventricular Cerliponase Alfa for CLN2 disease. *N Engl J Med*. 2018;378:1898–1907.

Footnotes and Financial Disclosures

Originally received: November 4, 2019.
Final revision: November 7, 2019.
Accepted: November 7, 2019.
Available online: November 13, 2019. Manuscript no. ORET-D-19-00251.

[1] UCL Institute of Ophthalmology, University College London, London, United Kingdom.

[2] Moorfields Eye Hospital, London, United Kingdom.

[3] Casey Eye Institute, Oregon Health & Science University, Portland, Oregon.

Supported by grants from the National Institute for Health Research Biomedical Research Centre at Moorfields Eye Hospital NHS Foundation Trust and UCL Institute of Ophthalmology, Onassis Foundation, Leventis Foundation, The Wellcome Trust (099173/Z/12/Z), Moorfields Eye Hospital Special Trustees, Moorfields Eye Charity, and Foundation Fighting Blindness (USA).

Financial Disclosure(s):
The author(s) have made the following disclosure(s): R.G.W. serves on advisory boards for the Foundation Fighting Blindness.

GAW and MG contributed equally and should be considered equivalent authors.

HUMAN SUBJECTS: Human subjects were included in this study. The human ethics committees at the Moorfields Eye Hospital approved the study. All research adhered to the tenets of the Declaration of Helsinki. All participants provided informed consent.

No animal subjects were used in this study.

Author Contributions

Conception and design: Wright, Georgiou, de Carvalho, Michaelides

Data collection: Wright, Georgiou, Oluonye

Analysis and interpretation: Wright, Georgiou, Robson, Holthaus, Pontikos, de Carvalho, Neveu, Weleber, Michaelides

Obtained funding: N/A

Overall responsibility: Wright, Georgiou, Robson, Ali, Kalhoro, Holthaus, Pontikos, Oluonye, Neveu, Weleber, Michaelides

Abbreviations and Acronyms:
ERG = electroretinography; **ERM** = epiretinal membrane; **ILM** = internal limiting membrane; **JNCL** = juvenile neuronal ceroid lipofuscinosis; **logMAR** = logarithm of the minimum angle of resolution; **mGCL** = macular ganglion cell layer; **NCL** = neuronal ceroid lipofuscinose; **NFL** = nerve fiber layer; **RPE** = retinal pigment epithelium; **SD** = standard deviation; **VA** = visual acuity.

Correspondence:
Michel Michaelides, MD (Res), FRCOphth, UCL Institute of Ophthalmology, 11-43 Bath Street, London, EC1V 9EL, UK. E-mail: michel.michaelides@ucl.ac.uk.